

<https://doi.org/10.1038/s42003-025-07925-z>

# Muscone-specific olfactory protein MjavOBP3 identified as the putative scent-marking pheromone in the Sunda pangolin (*Manis javanica*)



Zhongbo Yu<sup>1,2</sup>, Tao Meng<sup>3</sup>, Tengcheng Que<sup>4,5</sup>, Luyao Yu<sup>1,2</sup>, Yichen Zhou<sup>1,2</sup>, Meihong He<sup>4</sup>, Haijing Wang<sup>3</sup>, Yingjiao Li<sup>4</sup>, Liling Liu<sup>4</sup>, Wenjian Liu<sup>5</sup>, Yinliang Wang<sup>1,2</sup> & Bingzhong Ren<sup>1,2</sup>

Pangolins are mammals of important conservation interest, as only eight extant species remain globally and all are considered to be at risk of extinction. The Sunda pangolin (*Manis javanica*) is a burrowing and nocturnal animal with poor vision, thus intraspecies communication such as mating, warning, and scent-marking relies on olfaction. The specific pheromone involved in intraspecies communication in pangolins remains unknown. In this study, all odorant-binding proteins in Sunda pangolins are functionally expressed and screened against a panel of 32 volatiles that derived from the pangolin urine, feces, and anal gland secretions. Using reverse chemical ecology, we reveal that *M. javanica* odorant-binding protein 3 (MjavOBP3) possesses the highest binding affinity to muscone. We also apply a behavior-tracking assay to show that muscone is more attractive to male individuals than to females, suggesting that muscone is a scent-marking pheromone in the Sunda pangolin. Further, our molecular modeling shows that Tyr117 contributes the most to muscone binding, which is further validated by site-directed mutagenesis. These findings identify the scent-marking mechanism in pangolins, highlighting the potential of muscone to support monitoring and conservation of this endangered animal.

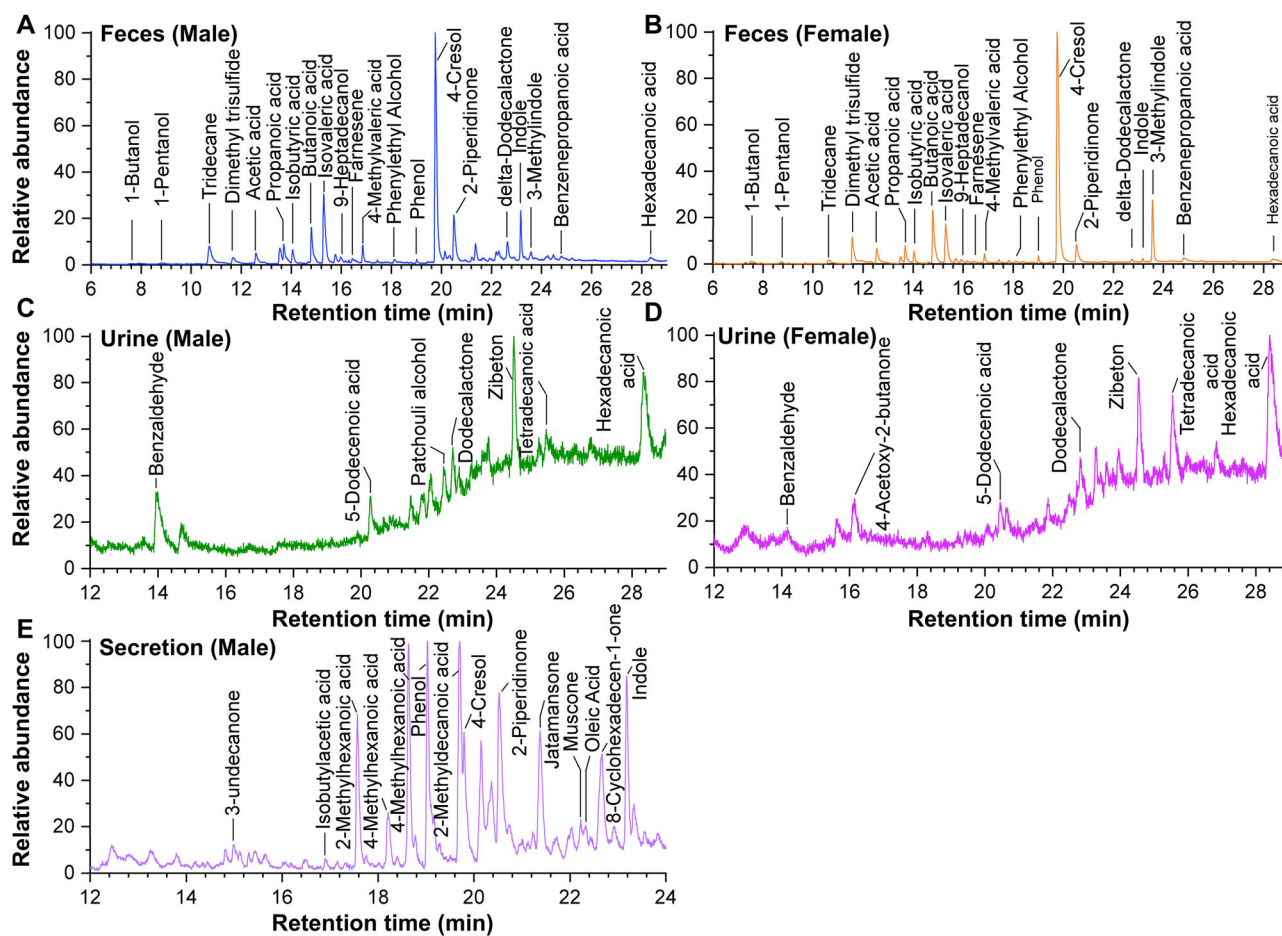
Scent-marking is one of the most conspicuous behaviors of mammals and other terrestrial vertebrates. It has long intrigued researchers from various disciplines<sup>1</sup>. Although the chemical composition, source, and behavioral effect of scent-marking are highly diverse among different taxa, it has been suggested to have four main functions: 1) attracting females to increase mating and reproductive success<sup>2</sup>; 2) advertising males' territory ownership and social dominance status<sup>3</sup>; 3) marking of food resources to increase foraging efficiency<sup>4</sup>; and 4) individual recognition among different species and populations<sup>5</sup>. In some cases, scent marking not only advertises the existence of the scent owners but also includes information about the individual's health, infections, age, sex, and mating state<sup>5–7</sup>. The source of the scent marking that is used by mammals is usually urine, feces, and glandular secretions<sup>8</sup>. For instance, Siberian wolves (*Canis lupus*) deposit feces at crossroads to increase the effectiveness of territory maintenance<sup>9,10</sup>, and

female Asian elephants (*Elephas maximus*) use urine to signal males of their readiness to mate<sup>11</sup>. Anal gland secretions are also used by some Carnivora, such as ferrets (*Mustela putorius furo*), meerkats (*Suricata suricatta*), domestic cats (*Felis catus*), and giant panda (*Ailuropoda melanoleuca*), and the scent that is emitted from their anal gland provides important information for intraspecies individual recognition<sup>12–15</sup>.

Pangolins belong to the family Manidae of the order Pholidota, closely related to the order Carnivora, and are represented by only eight extant species in the world<sup>16</sup>, including the Sunda pangolin *Manis javanica*. Due to the economic value of their meat, scales (attributed medicinal properties), and skins, enormous numbers of pangolins have been seized and traded in the black market, especially in Southeast Asia<sup>17</sup>. Currently, *M. javanica* is classified as a critically endangered species and is listed in Appendix II of the Convention on International Trade in Endangered Species of Wild Fauna

<sup>1</sup>Jilin Provincial Key Laboratory of Animal Resource Conservation and Utilization, School of Life Science, Northeast Normal University, Changchun, 130024, China.

<sup>2</sup>Key Laboratory of Vegetation Ecology, Ministry of Education, Northeast Normal University, Changchun, 130024, China. <sup>3</sup>Guangxi Forestry Inventory and Planning Institute, Nanning, 530011, China. <sup>4</sup>Guangxi Zhuang Autonomous Terrestrial Wildlife Rescue Research and Epidemic Diseases Monitoring Center, Nanning, 530003, China. <sup>5</sup>Faculty of Data Science City, University of Macau, Macau, 999078, China. e-mail: [wangyl392@nenu.edu.cn](mailto:wangyl392@nenu.edu.cn); [bzren@nenu.edu.cn](mailto:bzren@nenu.edu.cn)



**Fig. 1 | GC-MS analysis.** **A, B** Total ion chromatogram (TIC) of the volatiles from the feces of adult *M. javanica*. **C, D** TIC of the volatiles from the urine of adult *M. javanica*. **E** TIC of the volatiles from the anal gland secretion of male adult *M. javanica*.

and Flora (CITES)<sup>18</sup>. They are nocturnal mammals with a highly specialized diet, relying exclusively on ants and termites as their primary food sources. Genomic evidence shows that their olfactory receptor (*OR*) gene families are significantly expanded compared to their closest relatives, such as cats, dogs, and giant pandas, supporting the notion that they have a well-developed olfactory system<sup>19,20</sup>. Pangolins are generally solitary but they also have home ranges<sup>21</sup>, which are more distinguished in males. Male pangolins have been observed to display aggressive behavior toward each other to defend their home ranges, suggesting that they are territorial<sup>22</sup>. Most of the social interactions of *M. javanica* are believed to be scent-based and generally comprised of urine and anal glands secretions<sup>21</sup>; however, well-controlled behavioral experiments on *M. javanica* are still lacking, and our knowledge of the behaviors of *M. javanica* still relies on the observations from zoos and nature reserves.

Consequently, the reverse chemical ecology approach, involving the use of olfactory proteins as guides for identifying potential pheromones, may shed light on the communication behaviors of Sunda pangolin, and it is an effective tool for screening biologically active scents and clarifying their molecular mechanisms<sup>23</sup>. Among the olfactory proteins, odorant binding proteins (OBPs), which belong to the lipocalin family, were first discovered in the nasal cavities of cow<sup>24</sup>. Subsequently, OBPs have since been identified in mice, rats, domestic pigs, and giant pandas<sup>25</sup>. Currently, the main function of mammalian OBPs is the specific delivery of odorants to the olfactory receptors expressed in the olfactory epithelium (OE)<sup>25</sup>. Evidence suggests that these proteins might also be involved in scent markings. For instance, three OBPs were identified in the anal sac gland of dogs (*Canis lupus familiaris*) and are involved in the signal release and nasal mucosa reception of scent secretions<sup>26</sup>. Similarly, rodent urine also contains a class of lipocalins

that play a key role in individual recognition<sup>27</sup>. Although the genome of *M. javanica* was sequenced in 2017, at present, the functional expression of proteins of this kind has not been studied in this species. Moreover, the behavioral and molecular mechanisms of scent marking in Sunda pangolin remain elusive.

Consequently, we analyzed the *M. javanica* transcriptome from different tissues, and identified, cloned, and analyzed the expression of all three *M. javanica* OBPs (*MjavOBPs*). Based on the reverse chemical ecology approach, we screened these OBPs against a panel of volatiles from their urine, feces, and anal gland secretions with the aim to explore the scent-marking-related chemical signals. Additionally, the behavioral effect of the active ligands was evaluated using a behavioral tracking assay. Lastly, the key binding sites of the OBP-ligand complex were identified and verified by molecular modeling to clarify the structural-based selectivity of the *MjavOBPs*.

## Results

### Candidate volatiles were associated with scent marking

Forty-nine volatile compounds were identified through GC-MS analysis of urine, feces, and anal gland secretions associated with scent marking (Fig. 1; Supplementary Data 1). These included 21 fatty acids, seven ketones, seven alcohols, four esters, three alkanes, three aromatic compounds, and four other compounds. 4-Methylphenol and 3-methylindole, common volatiles in feces, were detected in the feces of both males and females (Fig. 1A, B). Additionally, ant-associated volatiles such as dimethyl trisulfide and farnesene were identified, which may be related to the pangolin's foraging habitats. The volatiles in the urine of both males and females included fatty acids such as hexadecanoic acid, tetradecanoic acid, and 9-hexadecanoic

**Table 1 | . Sunda pangolin lipocalins**

Protein family	Gene name	NR annotation	Length (nt)	Length (aa)	Molecular weight
Odorant binding protein (OBP)	MjavOBP1	Allergen Bos d 2-like isoform X1	522	173	19.34 kDa
	MjavOBP2	Odorant-binding protein 2b-like	519	172	19.40 kDa
	MjavOBP3	Odorant-binding protein-like	522	173	19.15 kDa
	MjavFABP1A1	Fatty acid-binding protein, liver	384	127	14.09 kDa
	MjavFABP1A2	Fatty acid-binding protein, liver	402	133	14.68 kDa
	MjavFABP2	Fatty acid-binding protein, intestinal	399	132	15.29 kDa
	MjavFABP3	Fatty acid-binding protein, heart	402	133	14.92 kDa
	MjavPMP2	Myelin P2 protein	402	133	14.87 kDa
	MjavFABP9	Fatty acid-binding protein 9-like	390	129	14.79 kDa
Fatty-acid-binding protein (FABP)	MjavFABP4	Fatty acid-binding protein, adipocyte	399	132	14.89 kDa
	MjavFABP5A1	Fatty acid-binding protein, epidermal	408	135	15.17 kDa
	MjavFABP5A2	Fatty acid-binding protein, epidermal	408	135	15.08 kDa
	MjavFABP6	Gastrotropin isoform X2	387	128	14.68 kDa
	MjavFABP7	Fatty acid-binding protein, brain	399	132	14.90 kDa
	MjavFABP12	Fatty acid-binding protein 12	462	153	17.17 kDa
	MjavRBP1	Retinol-binding protein 1	408	135	15.80 kDa
	MjavRBP2	Retinol-binding protein 2	282	93	10.73 kDa
Retinol binding protein (RBP)	MjavRBP4	Retinol-binding protein 4	594	197	22.54 kDa
	MjavRBP5	Retinol-binding protein 5	408	135	15.91 kDa
	MjavRBP7	Retinoid-binding protein 7 isoform X2	384	127	14.71 kDa
Beta-lactoglobulin (BLG)	MjavBLG1	Beta-lactoglobulin-1-like, partial	543	180	20.31 kDa
	MjavBLG2	Lactoglobulin-2	543	180	20.30 kDa
Cellular retinoic acid-binding protein (CRABP)	MjavCRABP1	Cellular retinoic acid-binding protein 1	414	137	15.57 kDa
	MjavCRABP2	Cellular retinoic acid-binding protein 2	417	138	15.72 kDa
Epididymal-Specific Lipocalin	MjavLCN6	Epididymal-specific lipocalin-6	498	165	17.88 kDa
	MjavLCN9	Epididymal-specific lipocalin-9 isoform X2	498	165	18.88 kDa
Apolipoprotein D	MjavAPOD	Apolipoprotein D	570	189	21.47 kDa
Orosomucoid	MjavORM1	Alpha-1-acid glycoprotein-like isoform X1	669	222	24.76 kDa
Prostaglandin D2 synthase	MjavPTGDS	Prostaglandin-H2 D-isomerase	576	191	21.18 kDa
Von Ebner's gland protein	MjavLCN1	Lipocalin-1-like	552	183	19.80 kDa
Neutrophil gelatinase-associated lipocalin	MjavLCN2	Neutrophil gelatinase-associated lipocalin	600	199	22.91 kDa
Salivary lipocalin protein	MjavSAL1	Minor allergen Can f 2-like	555	184	20.41 kDa
Human-specific lipocalin	MjavLCN15	Lipocalin-15 isoform X3	492	163	17.85 kDa
Complement component 8	MjavC8G	Complement component C8 gamma chain isoform X2	831	276	30.92 kDa

acid (Fig. 1C, D). The volatile components of anal gland secretions were similar to those found in feces, with both containing 4-methylphenol, phenol, and indole (Fig. 1E). Notably, muscone, which is the scent-marking pheromone in musk deer, and 8-cyclohexadecen-1-one, a volatile that has a similar chemical structure to muscone, were detected in the anal gland secretions (Supplementary Fig. S1). In our experiment, we found that only male pangolins can release approximately 3–5 mL of yellow, viscous anal gland secretions, while female individuals do not release any. Due to their endangered status, related research is limited, and the potential for muscone secretion in females remains unknown, requiring further investigation.

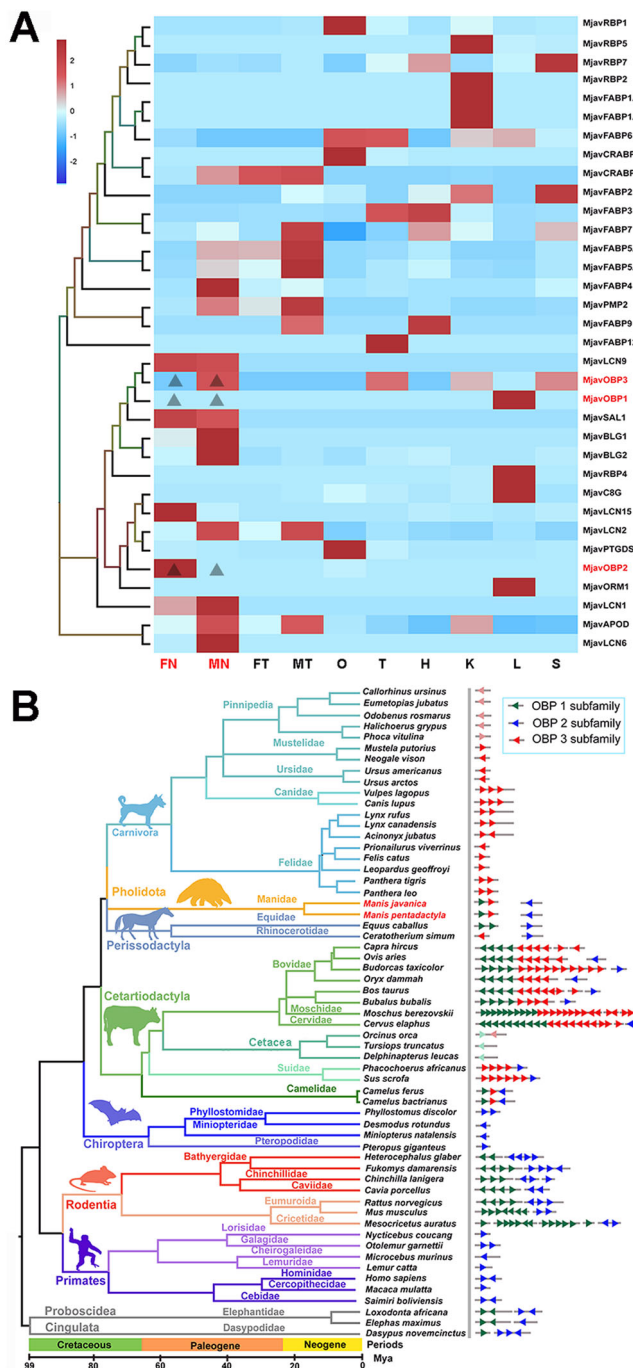
#### Muscone binds to MjavOBP3 with high affinity

A transcriptome analysis identified 34 lipocalin proteins, which belong to 14 different families, including three OBPs, 12 fatty acid-binding proteins, five retinoid-binding proteins, two  $\beta$ -lactoglobulins, and 12 other lipocalin proteins (Table 1). MjavOBP1 was only expressed in the liver, while MjavOBP2 and MjavOBP3 were highly expressed in the nasal cavity, suggesting their potential olfactory sensing roles (Fig. 2A; Supplementary Data 2).

Notably, MjavOBP3 was expressed exclusively in the nasal cavities of males, but not in females.

The homology analysis revealed that *MjavOBP1-3* belonged to in three different OBP subfamilies. Compared to previous studies<sup>26</sup>, a new OBP2 gene was identified in the Sunda pangolin. The number of OBPs highly varied among different species, ranging from 1 to 27 (Supplementary Fig. S2; Supplementary Data 2). The number of OBPs in Chiroptera, Primates, and Carnivora was close to that of pangolins, and the order Artiodactyla had up to 27 OBPs. In the Cetacea and Pinnipeds, all the OBPs appeared to be pseudogenes that contained a premature termination codon, suggesting the degeneration of their olfactory-sensing in underwater habits (Fig. 2B).

We then analyzed the functional expression of all three *MjavOBPs*. After purification, sodium dodecyl-sulfate polyacrylamide gel electrophoresis (SDS-PAGE) showed that the MjavOBPs had a target band at approximately 20 kDa (Supplementary Fig. S3, Supplementary Data 3), which was consistent with the predicted length of the amino acid sequence of those proteins. A liquid chromatography-mass spectrometry (LC-MS) analysis showed that the coverage rates of the measured amino acid



**Fig. 2 | Transcriptome and homology analysis.** **A** Expression profiles of lipocalins in *M.javanica*. (FN female nasal olfactory epithelium, MN male nasal olfactory epithelium, FT female tongue, MT male tongue, O ovary, T testis, H mixed sample of heart, K mixed sample of kidney, L mixed sample of liver, S mixed sample of stomach). The left side of the figure is a phylogenetic tree constructed using neighbor-joining for pangolin lipocalins, and the right side is the corresponding gene name. **B** Homology analyses of odorant binding protein (OBP) genes in 59 mammalian species. The gene tree constructed for OBPs using the maximum likelihood method is divided into three clades, corresponding to the OBP1-3 subfamily (Supplementary Fig. S2). The left side of the figure shows the species tree was generated using the TimeTree database<sup>52</sup>. The right side of the figure shows the number and location number of different types of OBPs in different color located on the chromosome. Light-colored arrows indicate pseudogenes. The animal silhouettes are sourced from the Phylopic.org website and are licensed under the Creative Commons Attribution-ShareAlike 3.0 Unported License. The license terms can be found at: <https://creativecommons.org/licenses/by-sa/3.0/>.

sequences ranged from 83% to 100% when compared with the reference sequences, validating the MjavOBPs that were purified (Fig. 3A–C, Supplementary Fig. S3).

Subsequently, three MjavOBPs were screened against a panel of 32 candidate scent-marking and plant volatiles using N-phenyl-1-naphthylamine (1-NPN) as a fluorescent reporter (Table 2, Fig. 3D–F; Supplementary Fig. S4). A competitive binding assay showed that both MjavOBP1 and MjavOBP2 bound to 2-undecanone with  $K_d$  values of  $56.55 \pm 4.20 \mu\text{M}$  and  $54.48 \pm 10.75 \mu\text{M}$ , respectively. Furthermore, MjavOBP1 had the best binding ability with the urinary volatile  $\delta$ -dodecalactone ( $38.74 \pm 2.04 \mu\text{M}$ ) and also bound weakly with other ligands, such as citral and 3-phenylpropionic acid. Then, MjavOBP2 had the highest binding affinity for skatole ( $40.83 \pm 8.93 \mu\text{M}$ ), and MjavOBP3 showed strong binding ( $\text{IC}_{50,2.23} \pm 0.80 \mu\text{M}$ ) with muscone, which is an anal gland secretion volatile, and MjavOBP3 also binds to other ketones, sesquiterpenes, and aldehydes, such as 3-undecanone,  $\beta$ -farnesene, and hexanal, with the  $\text{IC}_{50}$  value being higher than  $2.23 \mu\text{M}$  (Supplementary Data 3). In summary, muscone was found to exhibit an extremely strong affinity for MjavOBP3, providing direction for subsequent experiments.

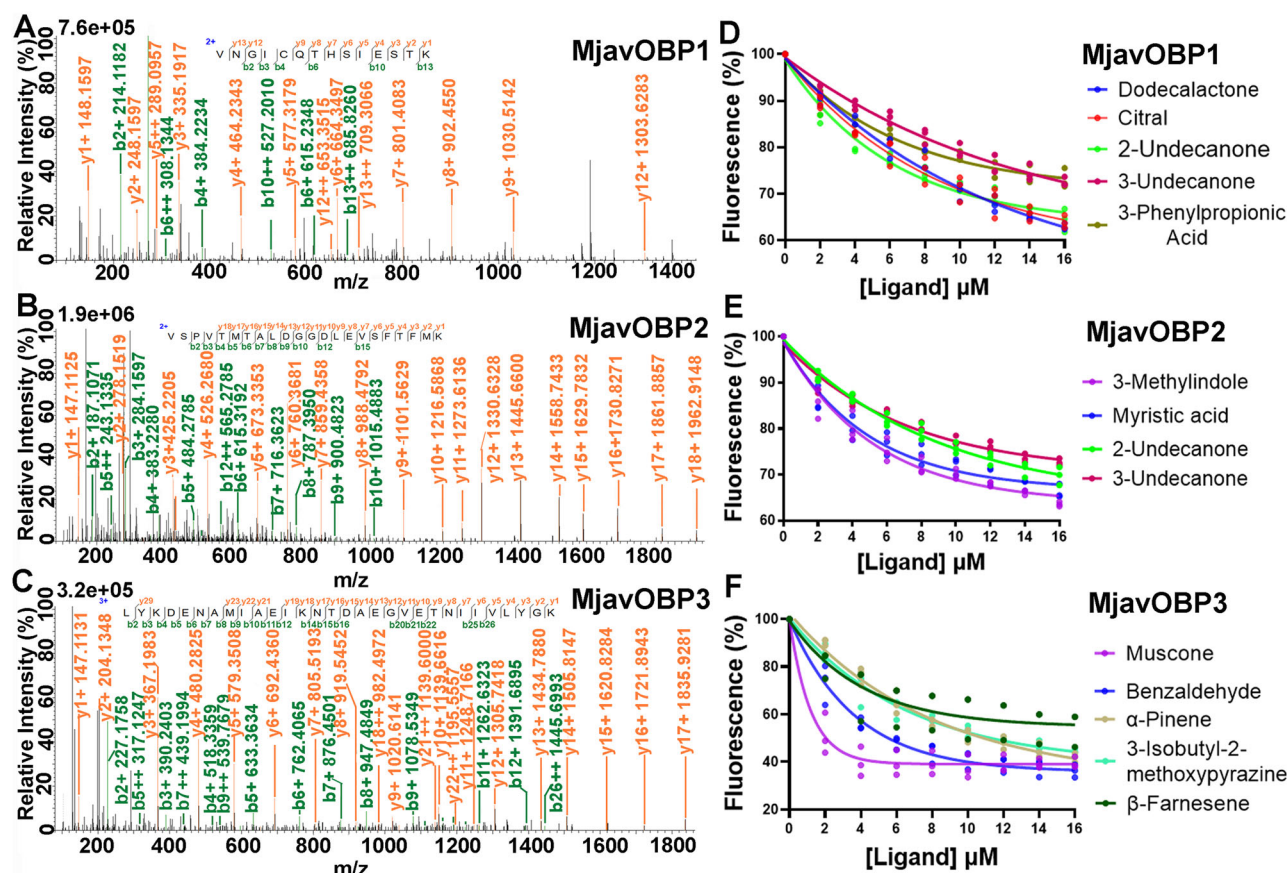
### Key binding sites for muscone on MjavOBP3

The 3D modeling and docking showed that muscone is wrapped in the center of a binding pocket on MjavOBP3 (Fig. 4A, B; Supplementary Fig. S5). Additionally, Tyr117 can form a hydrogen bond with muscone, with a molecular distance of  $2.8 \text{ \AA}$ , and the binding of muscone is also attributed to a Pi-alkyl interaction (Phe52), an alkyl interaction (Ile101), and Van der Waals forces (Glu68, Tyr81, and Tyr87; Fig. 4C). The 100 ns time-evolution root-mean-squared deviation (RMSD) test showed that the MjavOBP3-muscone complex systems experienced a large fluctuation during 0–14 ns and reached equilibrium at  $2.26 \text{ \AA}$  within 50 ns. The standard deviation of the RMSD after 50 ns was  $0.14 \text{ \AA}$ , indicating the stability and reliability of the MD trajectory (Fig. 4D). In the equilibrium phase, Tyr117 formed a hydrogen bond, and the other non-polar residues (Phe52, Glu68, Tyr81, Tyr87, and Ile101) formed Van der Waals forces and a (pi)-alkyl bond, which also contributed to the MjavOBP3-muscone interactions (Fig. 4E). The binding free energy of the MjavOBP3-muscone complex was predicted to be  $-39.42 \text{ kcal/mol}$  (Supplementary Data 4). Subsequently, the residues with a total energy contribution ( $\Delta G_{\text{bind}}$ ) exceeding  $-1.00 \text{ kcal/mol}$  were chosen for further validation (Fig. 4F), which included Tyr117, Phe52, Ile101, Glu68, Tyr81, Tyr87, and two negative control residues (Met97, inside the binding pocket; Lys130, far away from the binding pocket).

When compared with the wild type, the binding affinity of muscone in the four mutations (F52A, Y81A, Y87A, and Y117F) was significantly decreased ( $P < 0.01$ ; Fig. 5A–C; Supplementary Fig. S6, Supplementary Data 5), which shows that Y117F does not bind to muscone with a  $K_d$  value of  $116.78 \pm 4.41 \mu\text{M}$ . The fluorescence binding results were highly consistent with the modeling and docking predictions, indicating that the Phe52, Tyr81, Tyr87, and Tyr117 residues are crucial for the binding of muscone, and the Tyr117 residues contributed the most to the binding process.

The amino acids alignment on MjavOBP3 showed 16 conserved residues (indicated by \*) among its orthologues (Fig. 5D). The similarity of the homologous MjavOBP3 among the different species ranged from 28% to 90%, and the highest similarity was with its close relative, *Manis pentadactyla*. The above four key residues (Tyr117, Phe52, Tyr87, and Tyr81) were highly conserved between *M. javanica* and *M. pentadactyla*, suggesting a similar olfactory sensing pathway for muscone. Among the key binding residues, Phe52 (Pi-alkyl) and Tyr81 (Van der Waals force) were highly conserved among the mammals, indicating their crucial role in the OBP3 orthologues. In contrast, Tyr117 (Hydrogen bond) was only conserved in *M. javanica* and *M. pentadactyla*, suggesting that it contributes the most to the muscone binding and has a crucial role in specific sensing of muscone in pangolins.





**Fig. 3 | Sequencing analysis and ligand binding ability determination of three MjavOBPs.** A–C Mass spectrum of peptides from three MjavOBPs are shown, respectively. The fragments are reported in different colors depending on peptides present in *M. javanica* and corresponding b and y ion series. D–F Binding curves of

all MjavOBPs to different ligands. The ligand names are shown on the right of the curves with different colors, and binding affinity data are listed in Supplementary Data 3.

### Behavioral responses of the pangolins to muscone

Muscone was detected in the anal gland secretions of male pangolins and exhibited the strongest binding affinity for MjavOBP3. This finding led to further investigation of the behavioral responses of the Sunda pangolin to muscone. The results of the behavioral experiments showed that both male and female pangolins visited and stayed in the f5 area more frequently, where was the entrance of the resting place. After placing the control odor source (propylene glycol), both the males and females visited and stayed on the left side of the room more frequently, with neither males nor females showing any attraction to the odor source (Fig. 6A, C; Supplementary Movie S2 and S4). After the muscone was placed, the males could accurately recognize the muscone (area b8, Fig. 6 B, Supplementary Movie S3). Although no female activity was observed in the area b8, they exhibited distinct activity trajectories in the b6 and c6 areas near the odor source compared to the control group (Supplementary Movie S5). Each experiment was repeated 10 times and similar results were obtained.

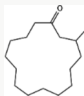
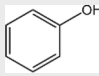
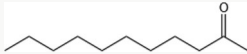


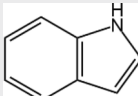
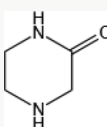

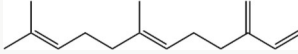
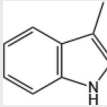
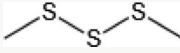
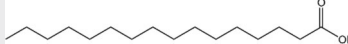
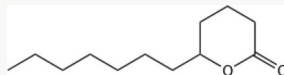
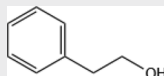
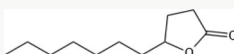
Then, the average staying time of the pangolins in each area was based on three males and three females (Fig. 6, Supplementary data 6). In the control group, the highest staying time of the males was in the order of f5 ( $45.09 \pm 12.46$  s), b2 ( $35.62 \pm 15.04$  s), and b1 ( $31.11 \pm 15.23$  s), while that for the females was in the order of f5 ( $32.56 \pm 5.79$  s), c2 ( $18.94 \pm 4.35$  s), and d2 ( $13.39 \pm 0.13$  s). The average staying time for both sexes in b8 was 0 (Fig. 6E, G), suggesting that neither the males nor females could identify the control odor. In the muscone group, the highest staying time for the males was for b8 ( $78.10 \pm 20.04$  s), and the staying time in the muscone area (b8) was significantly ( $p < 0.01$ ) higher than that of any of the other areas (Fig. 6F). In addition, the times spent by males investigating the muscone were significantly longer than those for the PG control (area b8,  $p = 0.004$ ,

Supplementary Fig. S7A). In contrast, the time spent by females in the muscone area was 0. However, compared to the control odor, females stayed longer near the muscone area (a6–d6), with significant differences showing in areas b6 ( $p = 0.023$ ) and c6 ( $p = 0.045$ , Supplementary Fig. S7B), indicating that females could also detect muscone. In summary, the behavioral tracking results showed that male pangolins exhibited a stronger preference for muscone compared to females.

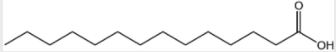
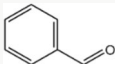
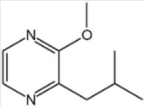
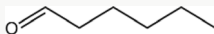
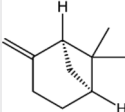
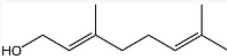

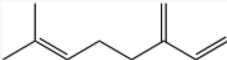

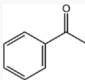
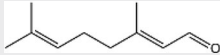
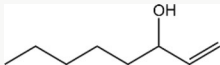

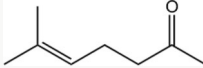
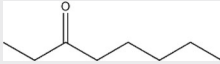

### Discussion

The volatile organic compounds (VOCs) that were identified from the urine, feces, and anal gland secretions of the pangolins were mainly carboxylic acids, ketones, and alcohols, which were followed by lactones and aldehydes. Among them, carboxylic acids, aldehydes, phenols, and indoles are often detected in mammal excretions<sup>28</sup> and these VOCs may not convey intraspecies information. Notably, some of the VOCs, such as δ-dodecalactone, farnesene, and muscone, are rare in nature or pangolin-specific, indicating their potential pheromone role. Specifically, δ-dodecalactone may act as a scent-marking signal in male Bengal tigers (*Panthera tigris*)<sup>29</sup>, and farnesene, which is derived from the urine of male mice, was shown to be a territory-marking pheromone<sup>30</sup>. Muscone is a rare VOC in mammal secretions, only four mammal species can synthesize and release muscone, namely, the musk deer, musk shrew, musk ox, and muskrat. These species share some common characteristics in that the muscone is synthesized and released primarily by male individuals, and is known to play a role in territory marking and female attraction<sup>31,32</sup>. Similarly, we found that male pangolins could also release muscone through their anal gland secretions. The food sources of pangolins (ants and termites) do not contain any muscone-relevant compounds<sup>33,34</sup>, indicating that there might be a specific

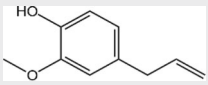

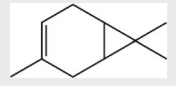
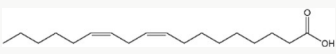
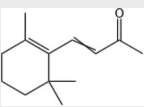
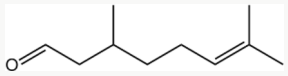
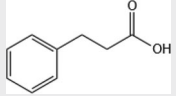
**Table 2 | Compounds used for functional verification of odorant binding proteins (OBPs) in Sunda pangolins**

Compound	Source	Cas number	Molecular structure	Purity	Company
Muscone	Secretion	541-91-3		97.0%	Aladdin
Phenol	Secretion	108-95-2		99.0%	Aladdin
2-Undecanone	Secretion	112-12-9		99.0%	Aladdin
3-Undecanone	Secretion	2216-87-7		≥85%	Aladdin
Oleic acid	Secretion	112-80-1		98.0%	Aladdin
Indole	Secretion feces	120-72-9		99.0%	Aladdin
2-Piperazinone	Secretion feces	5625-67-2		98.0%	Aladdin
Tridecane	Feces	629-50-5		98.0%	Aladdin
β-farnesene	Feces	18794-84-8		90.0%	Aladdin
3-methylindole	Feces	83-34-1		98.0%	Aladdin
Dimethyl trisulfide	Feces	3658-80-8		98.0%	Aladdin
Palmitic acid	Feces urine	57-10-3		97.0%	Aladdin
δ-Dodecalactone	Feces urine	713-95-1		98.0%	Aladdin
Phenethyl alcohol	Feces urine	60-12-8		99.0%	Aladdin
γ-Undecanolactone	Urine	104-67-6		98.0%	Aladdin

**Table 2 (continued) | Compounds used for functional verification of odorant binding proteins (OBPs) in *Sunda pangolins***

Compound	Source	Cas number	Molecular structure	Purity	Company
Myristic acid	Urine	544-63-8		98.0%	Aladdin
Benzaldehyde	Urine	100-52-7		99.5%	Aladdin
2-Isobutyl-3-methoxypyrazine	Habitat Volatiles	24683-00-9		99.0%	Sigma
Hexanal	Habitat Volatiles	66-25-1		99.0%	Aladdin
$\beta$ -Pinene	Habitat Volatiles	18172-67-3		98.0%	Rhawn
Geraniol	Habitat Volatiles	106-24-1		98.0%	Sigma
$\alpha$ -pinene	Habitat Volatiles	80-56-8		98.0%	Sigma
Myrcene	Habitat Volatiles	123-35-3		99.0%	Aladdin
Undecane	Habitat Volatiles	1120-21-4		97.0%	Aladdin
Acetophenone	Habitat Volatiles	98-86-2		99.5%	Aladdin
Citral	Habitat Volatiles	5392-40-5		97.0%	Aladdin
1-octen-3-ol	Habitat Volatiles	3391-86-4		98.0%	Aladdin
Nonanal	Habitat Volatiles	124-19-6		95.0%	Sigma
6-Methyl-5-hepten-2-one	Habitat Volatiles	110-93-0		99.0%	Sigma
3-Octanone	Habitat Volatiles	106-68-3		98.0%	Aladdin
Octanal	Habitat Volatiles	124-13-0		99.0%	Sigma

**Table 2 (continued) | Compounds used for functional verification of odorant binding proteins (OBPs) in Sunda pangolins**

Compound	Source	Cas number	Molecular structure	Purity	Company
Eugenol	Habitat Volatiles	97-53-0		99.0%	Sigma
Pentadecane	Habitat Volatiles	629-62-9		98.0%	Aladdin
3-Carene	Habitat Volatiles	13466-78-9		≥90%	Aladdin
Linoleic acid	Habitat Volatiles	60-33-3		95.0%	Aladdin
β-Lonone	Habitat Volatiles	14901-07-6		96.0%	Sigma
Citronellal	Habitat Volatiles	106-23-0		96.0%	Heowns
3-Phenylpropionic acid	Habitat Volatiles	501-52-0		99.0%	Aladdin

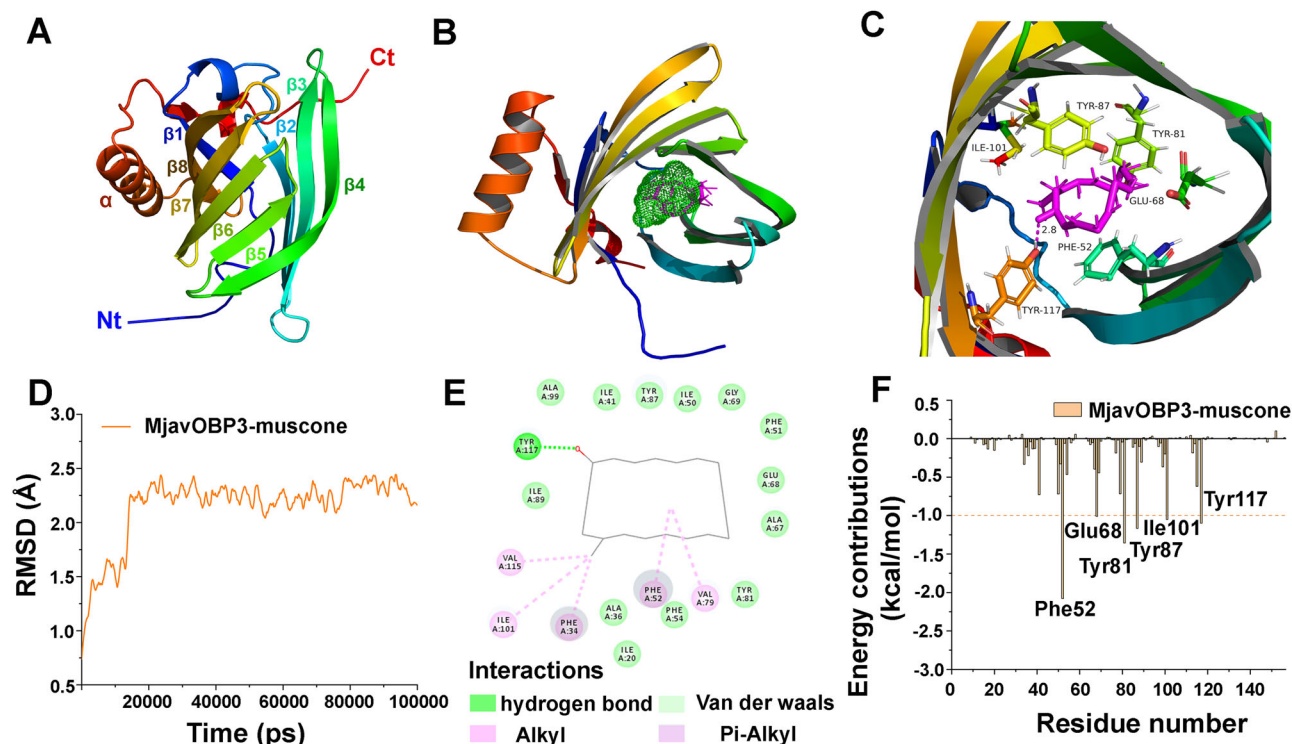
biosynthesis pathway for muscone in pangolins, which would also reflect their unique biological function. Notably, urine, feces, and anal gland secretions may also contain non-volatile compounds associated with scent marking; this requires further verification. For example, in mice, major urinary proteins (MUPs) have been demonstrated to enhance competitive scent-marking behaviors<sup>35</sup>.

The OBPs' main function is to increase the solubility of odorants and transport odorants to olfactory receptors (ORs) in a hydrophilic environment<sup>25</sup>. To date, verification of odorant-OR pairs in vitro experiments is limited and primarily focused on model mammals<sup>36,37</sup>. Ligand-binding experiments have been performed with OBPs of several mammal species<sup>25</sup>, the binding specificity between olfactory proteins and volatiles may pave the way for the identification of semiochemicals that are still unknown in mammals<sup>23,38</sup>. The present study demonstrated the presence of *OBP2* in the Sunda pangolin, *OBP2* has been found in other mammalian orders except for Carnivora. However, the specific role of those genes in chemical communication remains unknown. The number of *OBPs* varies greatly among the different animal groups; for instance, the number of *OBPs* in insects mainly ranges from 40 to 60<sup>39</sup>, while the number of *OBPs* in mammals is comparatively small. Our study showed that the number of *OBPs* in the orders Pholidota, Carnivora, Perissodactyla, Chiroptera, and Primates were only 1–3, and the reduction of *OBPs* in these species was likely due to an insufficient olfactory transport ability to varied environmental volatiles, which limited their function to pheromone carrying<sup>25</sup>. For example, a recent study showed that AimelOBP3 in giant pandas is bound with linear aldehydes, and they may be involved in pheromone recognition<sup>23</sup>. Pangolins are fossorial, and their vision quality is low but their olfactory system is well developed, and, thus, chemical signals play a key role in their intraspecies communications<sup>21</sup>. The fluorescence binding assay showed that MjavOBP3 had the highest binding affinity to muscone, suggesting that muscone has a putative pheromone-sensing role.

To further explore the behavioral effect of muscone on pangolins, a well-controlled behavioral assay was performed on this endangered species. The behavioral tracking assay indicated that the Sunda pangolins spent longer in areas distant from the propylene glycol control (b2-d2), possibly due to an aversion to propylene glycol<sup>40</sup>. Within the muscone group, male pangolins exhibited a stronger preference for muscone compared to females, which was consistent with the fact that MjavOBP3 is only expressed in the olfactory epithelium of males. Muscone is released by the anal glands of male Sunda pangolins, and the anal gland is a common organ in mammals, its main function is to synthesize anal gland secretions and lubricate the feces. However, in some cases, the anal gland is also responsible for territory marking and intraspecies recognition (such as in *Meles meles* and *Herpestes javanicus*)<sup>41,42</sup>. Male pangolins prefer to live in solitary, and they usually have a fixed living place with a home range of approximately 40 ha<sup>22</sup>. Field observations have shown that pangolins are territorial animals, and males sometimes fight with each other for territory. Considering that pangolins have poor vision but a well-developed olfaction, thus, territorial marking is believed to rely on chemical signals. Similar behavior was also observed in other Carnivora mammals, and they are close relatives to Pholidota. For example, *Crocuta crocuta* and *Canis lupus* use anal gland secretion for scent and territory marking<sup>43,44</sup>. The fluorescence binding assays showed that muscone is the best ligand for MjavOBP3, and it is a macrocyclic ketone that is composed of 15 carbons with a slow release and long-lasting aroma, which is consistent with the persistence characteristics of scent-marking pheromones<sup>45</sup>. Moreover, muscone is a rare chemical in nature and has only been detected in a few mammals, such as muskrats (*Ondatra zibethicus*) and musk deer, where it is used for scent marking<sup>31</sup>. Therefore, we hypothesized that muscone is a scent-marking pheromone in *M. javanica*.

Using the approach of reverse chemical ecology, we conducted the first screening for potential pheromones associated with scent marking in the





**Fig. 4 | Prediction of key sites in the MjavOBP3-muscone complex.** **A** The 3D structure of MjavOBP3 represents a barrel-like structure, mainly composed of 8  $\beta$ -sheets ( $\beta$ 1– $\beta$ 8) and 1  $\alpha$ -helix; **B** The predicted binding pocket is shown in green. The ligand muscone (dark pink) is tightly wrapped by the binding pocket; **C** 3D visual analysis of the binding mode of MjavOBP3 and muscone. Important amino acid residues and muscone are shown as baseballs, with hydrogen bonds represented by

pink dotted lines, and molecular distances are calculated; **D** The root-mean-square deviation (RMSD) curve of the MjavOBP3–muscone complex. **E** Protein–ligand interaction diagram of MjavOBP3 bound to muscone at steady state; **F** Total energy contribution of each amino acid residue in the MjavOBP3–muscone complexes. The residues with a total energy contribution of more than  $-1.00$  kcal/mol are indicated.

Sunda pangolin, thereby revealing the molecular mechanisms underlying its olfactory communication. The current conservation strategy would benefit from understanding how male pangolins communicate with each other via chemical signals at a molecular level. The discovery of scent-marking pheromones in pangolins could be used to monitor this endangered species<sup>46,47</sup>, and a scent-based pheromone trap could be developed for the observation and relocation of this endangered animal.

## Methods

### Ethics statement

All the animal procedures were approved by the ethics committee for animal experiments at the Terrestrial Wildlife Rescue and Epidemic Diseases Surveillance Center of Guangxi, and the recommended guidelines were followed (Supplementary Fig. S8). In brief, adult Sunda pangolins (*M. javanica*) were housed individually in pens consisting of an indoor house ( $1.6 \times 1.2$  m) and they were fed on a paste containing a mixture of ant powder, mealworms, eggs, apples, and carrots.

### Gas chromatography-mass spectrometry analysis

Feces, urine, and anal secretions of Sunda pangolins were collected in January. The individuals that were used in this study were three adult males and three adult females, and the detailed information for each individual is listed in Supplementary Data 7. The volatile samples were collected in a 10 mL bottle and adsorbed using a solid-phase microextraction syringe (Supelco 50/30  $\mu$ m DVB/CAR/PDMS, Manual Holder, 3pk, USA) for 30 min. The samples were analyzed using a GC-MS chromatograph (Agilent 6890 N/5973I, USA), and the temperature was maintained isothermally at  $80^\circ\text{C}$  for 3 min and increased to  $350^\circ\text{C}$  at a rate of  $10^\circ\text{C}/\text{min}$  for 27 min. High-purity helium was used as the carrier gas at a flow rate of 1 mL/min. The compounds in the analyzed samples were identified according to the NIST

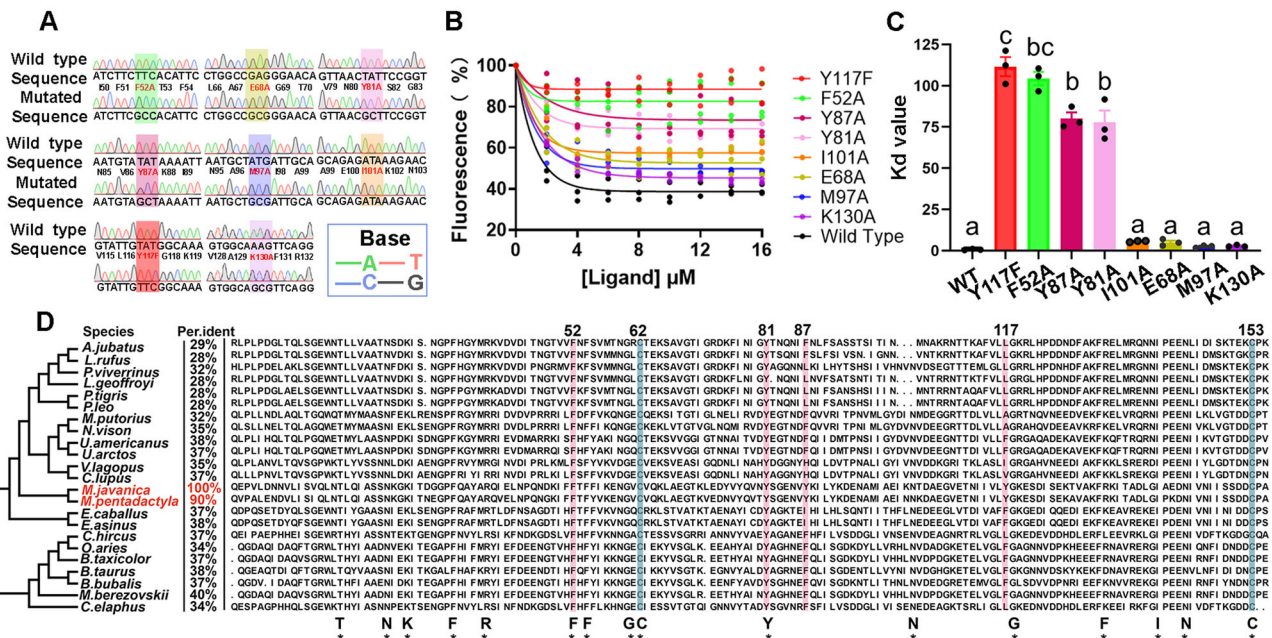
2014 mass spectral library. Three replicate measurements were conducted for each sample type.

### Transcriptome analysis

Frozen samples of three male and three female pangolins were used to extract the total RNA. Ten tissues from the frozen samples mentioned above were used for RNA sequencing, including the nasal olfactory epithelium of the male and female, tongue of the male and female, ovary, testis, and sex-mixed samples of the heart, kidney, liver, and stomach. The total RNA was extracted using TRIzol reagent (Invitrogen, USA), and the complementary DNA libraries were constructed using magnetic beads and Illumina's NEBNext Ultra RNA Library Prep Kit (Illumina, USA) from Biomarker Technologies (Beijing, China). RNA sequencing was performed on an Illumina HiSeq 2000 PE150 platform (Illumina, San Diego, CA, USA). The raw data were filtered to remove adapter-containing, poly-N, and low-quality reads were filtered from the raw data using custom Perl scripts. The Q20 and Q30 values, GC content, and sequence duplication levels of the clean data were then assessed. Transcriptome assembly was performed using Trinity (version r20131110) with default settings<sup>48</sup>, and clustering was performed using the Trinity-cluster-with-id-com PI. The genome sequence of *M. javanica* (GCF\_014570535.1) served as the reference for annotations. Gene functions were annotated using various databases including NR, Pfam, KOG/COG/eggNOG, Swiss-Prot, KEGG, and GO. Then, Fragments Per Kilobase of transcript per Million mapped reads (FPKM) values were normalized by tissue using the Hplot online analysis platform, and clustering was performed using Ward. D2<sup>49</sup>.

### Homology analysis

The homology analysis was conducted using all OBP genes from 59 mammalian species. Among these, the OBP genes of 21 species were



**Fig. 5 | Verification of key sites of MjavOBP3-muscone complex.** **A** Target site in the MjavOBP3 gene (wild type) and results obtained from the mutagenesis of MjavOBP3 through site-directed mutagenesis, and bases A, T, C and G are represented by green, pink, blue and black respectively, and the eight mutation positions are represented by different color; **B** Binding curves of MjavOBP3 mutants to muscone. The lines (different colors) represent the different mutants, and the line (black) represents the wild type (WT); **C** Comparison of the binding affinities, which are indicated by  $K_d$  value, of MjavOBP3 WT and mutants to muscone, respectively.

Data are means  $\pm$  S.E.M. The significant differences were compared using one-way analysis of variance (ANOVA) with Tukey's honestly significant difference and indicated by different lowercase letters ( $p < 0.01$ ,  $n = 3$ ); **D** Comparison of the amino acid sequence similarity of MjavOBP3 homologous proteins. The sequence similarity is expressed by per ident. Asterisks (\*) indicate the same amino acids in all proteins. Conserved cysteines involved in the formation of disulfide bridges are shown in light blue, while key binding sites in MjavOBP3 for muscone are shown in light pink.

referenced from the research of Sunita Janssenswillen<sup>26</sup>, while those of the remaining 38 species were retrieved from the NCBI database. A total of 243 OBP genes were aligned using MAFFT v7<sup>50</sup>, and a maximum likelihood (ML) phylogenetic tree was constructed with the "One Step Build a ML Tree" module in TBtools-II v2.199<sup>51</sup> using default settings. Additionally, the species tree was generated using the TimeTree of Life database<sup>52</sup>. The trees were visualized with software FigTree v1.4.2.

### Gene cloning, expression, and purification

The open reading frame of MjavOBP1-3 was obtained by polymerase chain reaction (PCR) with specific primers that were designed by Primer Premier 5.0 (PREMIER Biosoft International, USA; Supplementary Table S1) with 2 $\times$  TransTaq HiFi PCR SuperMix I (Transgen Bio, China), and they were subcloned to pET30a (Novagen, Germany) between EcoRI and XhoI (NEB, USA) using a pEASY-Basic Seamless Cloning and Assembly Kit (Transgen Bio, China). The plasmids containing the target OBPs were subsequently transformed into BL21(DE3) competent cells and induced by 1 mM isopropyl  $\beta$ -D-1-thiogalactopyranoside (IPTG) at 34  $^{\circ}$ C for 10 h. The protein expression was checked using 15% SDS-PAGE and loaded onto a Ni-TED 6FF pre-packed chromatography column (Sangon Bio, China) in a High-Performance Liquid Chromatography system (AKTA pure, Sweden). The His tag was removed by Recombinant Bovine Enterokinase (Sangon Bio, China). Site-directed mutagenesis was achieved by using the Fast Mutagenesis System Kit (TransGen, China), with primers designed by Primer Premier 5.0 (Supplementary Table S1).

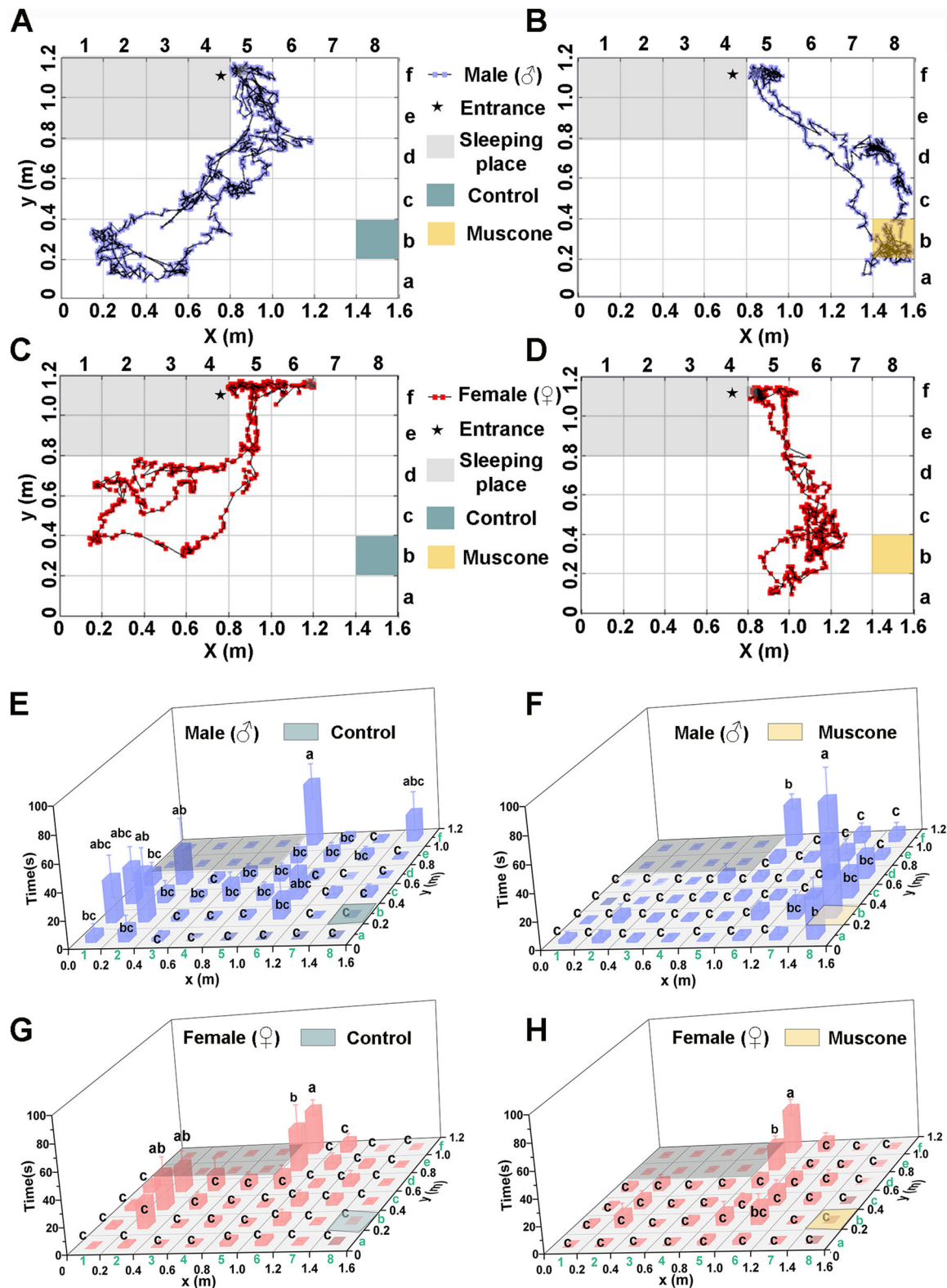
### Liquid chromatography-mass spectrometry analysis

The LC-MS was conducted according to Bortolussi et al. with a few modifications<sup>53</sup>. In brief, the gel was destained, washed, alkylated, and trypsinized. The samples were then desalted with a Zip-TipC18 column (Sigma Aldrich, USA) and eluted with a 67% acetonitrile solution containing 2% formic acid. The protein sample was analyzed by a nano LC-ESI-

Q Orbitrap tandem mass spectrometry (MS/MS) platform that consisted of the Dionex Ultimate 3000 HPLC RSLC nano system (Thermo Fisher Scientific, USA) and Q-Exactive Plus mass spectrometer (Thermo Fisher Scientific) mounted to a Nanoflex ion source (Thermo Fisher Scientific). The sample was first bound to a C18 Reversed Phase Column (Acclaim PepMap RSLC, 75  $\mu$ m  $\times$  150 mm, 2  $\mu$ m 100  $\text{\AA}$ ; Thermo Fisher Scientific) and eluted by gradient acetonitrile (from 0% to 80% over 80 min) containing 0.1% formic acid at 1 mL/min. The mass spectrometer was operated under the data-dependent analysis mode (MS1 scan resolution: 70,000; scanning range: 350–2000 m/z), which was followed by an MS/MS scan of the ten most abundant ions in high-energy collisional dissociation mode (maximum ion injection time: 50 ms; collision energy: 28 eV; dynamic exclusion: 25 s). Finally, the mass spectrum was converted into mgf format using ProteoWizard 3.0 software<sup>54</sup> and imported into Mascot v. 2.6.1 (Matrix Science, UK) for protein identification. The settings were as follows: database, uniprot; enzyme, trypsin; maximal number of missed cleavages, 1; MS tolerance, 20 ppm; MS/MS tolerance, 0.05 Da; protein score,  $\geq 95\%$ ).

### Fluorescence binding assays

The reaction was conducted in a 2 mL transparent quartz cell (Hellma, Germany). A mixture was constructed of 2  $\mu$ M protein dissolved in 50 mM Tris-HCl (pH 7.4) and 2  $\mu$ M probe 1-NPN dissolved in 50 mM Tris-HCl (pH 7.4), ligands were dissolved in methanol eight times to ensure the final content of the ligands was 2–16  $\mu$ M under a Fluoromax-4 spectrofluorometer (HORIBA Jobin Yvon, USA), and they were added to this mixture. Then, 1-NPN was used as a fluorescent reporter. The excitation wavelength was set to 337 nm, and the emission spectrum was recorded between 380 and 450 nm under an emission slit of 5 nm. The dissociation constants of the competitors were calculated using the equation  $K_d = IC_{50} / (1 + [1-NPN]/K_{1-NPN})$ , where  $IC_{50}$  is the concentration of ligands representing 50% of the initial fluorescence value of 1-NPN, [1-NPN] is the free concentration of 1-NPN, and  $K_{1-NPN}$  is the dissociation



**Fig. 6 | Preferential behavioral responses of female and male pangolins to muscone.** A–D Muscone odor or control odor (propylene glycol) was placed in area b8, and the behavioral trajectories of pangolins to control odors and muscone were recorded separately, ★ represents the entrance, the control odor is indicated in cyan with muscone shown in yellow, blue dots represent males, red dots represent females; E–H The time spent by the six pangolins in different areas of the room after

placement of the control odor or muscone. Blue histograms represent males and red histograms represent females. Bars indicate the mean time that a pangolin spent investigating each test sample within a 5-min period,  $\pm$ S.E.M. Different lowercase letters indicate significant differences with Duncan's multiple range test at the 0.01 level.



constant of the complex protein/1-NPN<sup>23</sup>. GraphPad Prism 9.0 software (GraphPad by Dotmatics, USA) was used for the  $K_d$  calculation.

### Molecular modeling and docking of MjavOBP3

The three-dimensional structure of MjavOBP3 was predicted using the AlphaFold2 platform based on the amino acid sequence<sup>55</sup>, and the highest score model was selected from the top five. The topology of the protein model was optimized by Amber 20<sup>56</sup> and the stereochemical quality of the modeled protein structure was verified by the PROCHECK method. Next, Sybyl v7.3 (Tripos, USA) was applied to calculate the interaction between the protein and ligand; the muscone was energy minimized, then it was docked to MjavOBP3 with “auto” binding cavity settings, and the total score was used to evaluate the binding affinity of the ligand to the target protein. Finally, the modeling and docking results were visualized by PyMOL (DeLano Scientific LLC).

### Molecular dynamic simulation and site-directed mutagenesis

The topology fields of the ligand and protein were generated under the AMBER ff14SB force field and general AMBER force field in Amber 20 software, respectively, and then the complex was immersed in a cubic box with TIP3P water molecules. Then, Na<sup>+</sup> was added to neutralize the entire system, and the energy of the complex was minimized by the steepest descent and conjugate gradient methods. Next, the system was heated from 0 to 300 K and the MD simulations were performed at constant 300 K and 1.0 Atmos for 100 ns using the PMEMD module. The RMSD of MjavOBP3-muscone was calculated to assess the equilibrium of the MD trajectories. The binding free energy between the residues and muscone was calculated using the Molecular Mechanics Poisson-Boltzmann Surface Area method<sup>57</sup>. The hydrogen bonding sites and the residues that contributed more than −1.00 kcal/mol to the binding free energy were selected for the mutagenesis validation.

### Behavioral tracking

Considering that Sunda pangolins are non-seasonal breeders<sup>22,58,59</sup>, the behavioral experiments were conducted from July to November (Supplementary data 7). The experiment was conducted during the peak activity period of the six pangolins (20:00–02:00) in a 1.6 × 1.2 m breeding room. The room was artificially divided into 48 small regions (20 × 20 cm), enabling recording of the visiting time of different areas of the room. Then, 450 µg of muscone dissolved in 40 µL of propylene glycol was used as the odor stimulus, with pure propylene glycol was used as a negative control<sup>60</sup>. The stimulus was added to an ethanol-cleaned plastic round box (2.4 cm diameter, 1.2 cm height) and placed at the corner of the room, and the behavior of the pangolins was recorded as soon as they left the resting area. A two-day interval was used between each experiment to avoid conditional reflex effects. The behaviors were recorded using an infrared camera (CuddeSafe J Series, Model 3525A) under dark conditions, with at least three technical replicates for the six individuals mentioned above. After recording, the behavioral path of the pangolins was tracked by the position of their noses with Tracker 6.1.5 software (Supplementary Movie S1). The visiting frequency was calculated using the average staying time in each region.

### Statistics and reproducibility

One-way analysis of variance (ANOVA) with Tukey’s honestly significant difference ( $p < 0.01$ ,  $n = 3$ ) test to analyze the significant differences in muscone affinity between the MjavOBP3 WT and mutants. In the behavioral assay, Duncan’s multiple range test ( $p < 0.01$ ,  $n = 10$ ) was used to perform multiple comparisons between the time spent in the odor source area (b8) and other areas. Differences in the investigation time between the control and muscone groups were analyzed using a paired Student’s  $t$  test ( $*p < 0.05$ ,  $**p < 0.01$ ,  $***p < 0.001$ ,  $n = 10$ ), with  $p$ -values corrected using the Benjamini–Hochberg (BH) method. All statistical analyses were conducted using SPSS v25.0 (IBM Corp., Armonk, NY, USA) and visualized with GraphPad Prism v8.0 (GraphPad Software, San Diego, CA, USA).

### Reporting summary

Further information on research design is available in the Nature Portfolio Reporting Summary linked to this article.

### Data availability

The transcriptome data have been deposited into the NCBI SRA database (accession numbers: SRR31641151-3, SRR23375506-17, SRR31645651, SRR31646405, SRR31656896, SRR31657344, SRR31660075, SRR31662187, SRR31643467). The source data supporting all the main figures are presented as a Supplementary Data file and archived in the figshare database (<https://doi.org/10.6084/m9.figshare.28427711.v1>)<sup>61</sup>. The Supplementary Movie is also stored in the figshare database (<https://doi.org/10.6084/m9.figshare.28432433.v1>). All other data are available from the corresponding author upon reasonable request.

Received: 24 September 2024; Accepted: 11 March 2025;

Published online: 26 March 2025

### References

1. Ralls, K Mammalian Scent Marking: Mammals mark when dominant to and intolerant of others, not just when they possess a territory. *Science* **171**, 443–449 (1971).
2. Thonhauser, KE et al. Scent marking increases male reproductive success in wild house mice. *Anim. Behav.* **86**, 1013–1021 (2013).
3. Gosling, LM & Roberts, SC Scent-marking by male mammals: cheat-proof signals to competitors and mates. *Adv. Study Behav.* **30**, 169–217 (2001).
4. Thompson, CL et al. Do common marmosets (*Callithrix jacchus*) use scent to communicate information about food resources?. *Folia Primatologica* **89**, 305–315 (2018).
5. Berns, GS, Brooks, AM & Spivak, M Scent of the familiar: An fMRI study of canine brain responses to familiar and unfamiliar human and dog odors. *Behavioural Process.* **110**, 37–46 (2015).
6. Zala, SM, Potts, WK & Penn, DJ Scent-marking displays provide honest signals of health and infection. *Behav. Ecol.* **15**, 338–344 (2004).
7. Ferkin, MH Age affects over-marking of opposite-sex scent marks in meadow voles, *Microtus pennsylvanicus*. *Ethology* **116**, 24–31 (2010).
8. Wyatt, T. D. *Pheromones and animal behaviour: communication by smell and taste*. (Cambridge university press, 2003).
9. Peters, R. & Mech, L. D. Scent-marking in wolves. *Wolf Man* **7**, 133–147 (1978).
10. Barja, I, de Miguel, FJ & Bárcena, F The importance of crossroads in faecal marking behaviour of the wolves (*Canis lupus*). *Naturwissenschaften* **91**, 489–492 (2004).
11. Rasmussen, LEL et al. Insect pheromone in elephants. *Nature* **379**, 684–684 (1996).
12. Clapperton, BK, Minot, EO & Crump, DR An olfactory recognition system in the ferret *Mustela furo* L. (Carnivora: Mustelidae). *Anim. Behav.* **36**, 541–553 (1988).
13. Leclaire, S et al. Odour-based kin discrimination in the cooperatively breeding meerkat. *Biol. Lett.* **9**, 1054 (2013).
14. White, AM, Swaisgood, RR & Zhang, H Chemical communication in the giant panda (*Ailuropoda melanoleuca*): the role of age in the signaller and assessor. *J. Zool.* **259**, 171–178 (2003).
15. Miyazaki, T et al. Olfactory discrimination of anal sac secretions in the domestic cat and the chemical profiles of the volatile compounds. *J. Ethol.* **36**, 99–105 (2018).
16. Lv, X et al. Diverse phylogenomic datasets uncover a concordant scenario of laurasiatherian interordinal relationships. *Mol. Phylogenetics Evolution* **157**, (2021). 107065.
17. Van Thai, N et al. Tapping into Local Knowledge to Help Conserve Pangolins in Viet Nam. *Workshop on Trade and Conservation of pangolins Native South and Southeast Asia* **6**, 163–168 (2009).



18. Inskipp, T. & Gillett, H. J. Checklist of CITES species and annotated CITES appendices and reservations: a reference to the appendices to the Convention on International Trade in Endangered Species of Wild Fauna and Flora, <https://coilink.org/20.500.12592/vq8sj> (2005).
19. Choo, SW et al. Pangolin genomes and the evolution of mammalian scales and immunity. *Genome Res.* **26**, 1312–1322 (2016).
20. Policarpo, M et al. Diversity and evolution of the vertebrate chemoreceptor gene repertoire. *Nat. Commun.* **15**, 1421 (2024).
21. Challender, D. W. S., Nash, H. C. & Waterman, C. *Pangolins: science, society and conservation* (Academic Press, 2019).
22. Lim, NTL & Ng, PKL Home range, activity cycle and natal den usage of a female Sunda pangolin *Manis javanica* (Mammalia: Pholidota) in Singapore. *Endanger. Species Res.* **4**, 233–240 (2008).
23. Zhu, J., et al. Reverse chemical ecology: olfactory proteins from the giant panda and their interactions with putative pheromones and bamboo volatiles. *Proc. National Acad. Sci.* **114**, E9802–E9810 (2017).
24. Pelosi, P et al. Binding of [3H]-2-isobutyl-3-methoxypyrazine to cow olfactory mucosa. *Chem. Senses* **6**, 77–85 (1981).
25. Pelosi, P & Knoll, W Odorant-binding proteins of mammals. *Biol. Zews* **97**, 20–44 (2022).
26. Janssenswillen, S et al. Odorant-binding proteins in canine anal sac glands indicate an evolutionarily conserved role in mammalian chemical communication. *BMC Ecol. Evol.* **21**, 1–16 (2021).
27. Hurst, JL et al. Individual recognition in mice mediated by major urinary proteins. *Nature* **414**, 631–634 (2001).
28. Burger, BV Mammalian semiochemicals. *Chem. Pheromones Other Semiochem. II* **240**, 231–278 (2005).
29. Burger, BV et al. Chemical characterization of territorial marking fluid of male Bengal tiger, *Panthera tigris*. *J. Chem. Ecol.* **34**, 659–671 (2008).
30. Harvey, S, Jemiolo, B & Novotny, M Pattern of volatile compounds in dominant and subordinate male mouse urine. *J. Chem. Ecol.* **15**, 2061–2072 (1989).
31. Ward, JP & van Dorp, DA The animal musks and a comment of their biogenesis. *Experientia* **37**, 917–922 (1981).
32. Watanabe, I. Odor components from musk glands of the house musk shrew. In: *Suncus Murinus* (ed. Kondo, K.) (Japan Scientific Societies Press, 1985).
33. Brophy, J. J., et al. Volatile constituents of two species of Australian formicine ants of the genera *Notoncus* and *Polyrhachis*. *Insect Biochem.* **12**, 215–219 (1982).
34. Mitaka, Y et al. Chemical identification of an aggregation pheromone in the termite *Reticulitermes speratus*. *Sci. Rep.* **10**, 7424 (2020).
35. Mucignat-Caretta, C & Caretta, A Urinary chemical cues affect light avoidance behaviour in male laboratory mice, *Mus musculus*. *Anim. Behav.* **57**, 765–769 (1999).
36. Mombaerts, P Genes and ligands for odorant, vomeronasal and taste receptors. *Nat. Rev. Neurosci.* **5**, 263–278 (2004).
37. Shirasu, M et al. Olfactory receptor and neural pathway responsible for highly selective sensing of musk odors. *Neuron* **81**, 165–178 (2014).
38. Zaremska, V et al. Reverse chemical ecology suggests putative primate pheromones. *Mol. Biol. Evol.* **39**, msab338 (2022).
39. Gong, D-P et al. The odorant binding protein gene family from the genome of silkworm, *Bombyx mori*. *BMC Genomics* **10**, 1–14 (2009).
40. Inagaki, H et al. The effect of vapor of propylene glycol on rats. *Chem. Senses* **35**, 221–228 (2010).
41. Davies, JM, Shepherdson, DJ & Roper, TJ Scent Marking with Faeces and Anal Secretion in the European Badger (*Meles Meles*): Seasonal and Spatial Characteristics of Latrine Use in Relation to Territoriality. *Behaviour* **97**, 94–117 (1986).
42. Kusuda, S et al. Induced estrus in female small Asian mongooses (*Herpestes javanicus*) for the purpose of controlling invasive alien species in Okinawa Island. *Mammal. Study* **35**, 217–219 (2010).
43. Dorrigiv, I, Hadian, M & Bahrman, M Comparison of volatile compounds of anal sac secretions between the sexes of domestic dog (*Canis lupus familiaris*). *Vet. Res. Forum* **14**, 3 (2023).
44. Drea, CM et al. Responses to olfactory stimuli in spotted hyenas (*Crocuta crocuta*): II. Discrimination of conspecific scent. *J. Comp. Psychol.* **116**, 342 (2002).
45. Apps, P, Mmualefe, L & McNutt, JW Identification of volatiles from the secretions and excretions of African wild dogs (*Lycaon pictus*). *J. Chem. Ecol.* **38**, 1450–1461 (2012).
46. Kerley, LL & Salkina, GP Using scent-matching dogs to identify individual Amur tigers from scats. *J. Wildl. Manag.* **71**, 1349–1356 (2007).
47. Campbell-Palmer, R & Rosell, F The importance of chemical communication studies to mammalian conservation biology: a review. *Biol. Conserv.* **144**, 1919–1930 (2011).
48. Grabherr, MG et al. Full-length transcriptome assembly from RNA-Seq data without a reference genome. *Nat. Biotechnol.* **29**, 644–652 (2011).
49. Li, J et al. Hiplot: a comprehensive and easy-to-use web service for boosting publication-ready biomedical data visualization. *Brief. Bioinforma.* **23**, bbac261 (2022).
50. Katoh, K & Standley, D MAFFT multiple sequence alignment software version 7: improvements in performance and usability. *Mol. Biol. Evol.* **30**, 72–80 (2013).
51. Chen, C et al. mTBtools-II: A “one for all, all for one” bioinformatics platform for biological big-data mining. *Mol. Plant* **16**, 1733–1742 (2023).
52. Kumar, S., et al. TimeTree 5: An Expanded Resource for Species Divergence Times. *Mol. Biol. Evol.* **39**, msac174 (2022).
53. Bortolussi, G et al. Impairment of enzymatic antioxidant defenses is associated with bilirubin-induced neuronal cell death in the cerebellum of Ugt1 KO mice. *Cell Death Dis.* **6**, 5 (2015).
54. Chambers, MC et al. A cross-platform toolkit for mass spectrometry and proteomics. *Nat. Biotechnol.* **30**, 10 (2012).
55. Jumper, J et al. Highly accurate protein structure prediction with AlphaFold. *Nature* **596**, 583–589 (2021).
56. Case, D. A. et al. AMBER 2021 software, <https://ambermd.org/CiteAmber.php> (University of California, San Francisco, CA, 2021).
57. Feig, M et al. Performance comparison of generalized born and Poisson methods in the calculation of electrostatic solvation energies for protein structures. *J. Computational Chem.* **25**, 265–284 (2004).
58. Zhang, F et al. Reproductive parameters of the Sunda pangolin, *Manis javanica*. *Folia Zoologica* **64**, 129–135 (2015).
59. Yan, D et al. Specific mating behavior of Malayan pangolin (*Manis javanica*) in captivity. *Sci. Rep.* **13**, 8592 (2023).
60. Horio, N., et al. Contribution of individual olfactory receptors to odor-induced attractive or aversive behavior in mice. *Nat. Commun.* **10**, 209 (2019).
61. Yu, Z. et al. Muscone-specific olfactory protein MjavOBP3 identified as the putative scent-marking pheromone in the Sunda pangolin (*Manis javanica*). figshare. Dataset. <https://doi.org/10.6084/m9.figshare.28427711.v1> (2025).

## Acknowledgements

We thank all the reviewers for comments on the manuscript and Yuxin Zhou, Xiaoyan Zhu and Haoqin Ke for their help with molecular biology experiments. As well as MJEditor ([www.mjeditor.com](http://www.mjeditor.com)) for providing English editing services during the preparation of this manuscript. This study was funded by the National Key Research and Development Program of China (No.2023YFE0113600).

## Author contributions

Z.Y. methodology; software; validation; formal analysis; investigation; data curation; writing—original draft preparation; writing—review and editing; visualization. T.M. software; validation; investigation; L.Y. investigation; data curation. Y.Z. software; validation. Tengcheng Que, formal analysis, data curation. H.W. investigation, visualization. M.H. investigation, data curation. Y.L. validation; investigation. L.L. software; formal analysis. W.L. software; data curation. Y.W. Conceptualization; validation; investigation; resources; writing—review and editing; supervision; project administration. B.R.

conceptualization; validation; investigation; resources; writing—review and editing; supervision; project administration; funding acquisition. All authors have read and agreed to the published version of the manuscript.

### Competing interests

The authors declare no competing interests.

### Ethics approval

All protocols for animal management were approved by the Ethics Committee of the Terrestrial Wildlife Rescue and Epidemic Diseases Surveillance Center of Guangxi (CLS-EAW-2020-05). The authors conformed with the Helsinki Declaration of 1975 (as revised in 2008) concerning Human and Animal Rights.

### Additional information

**Supplementary information** The online version contains supplementary material available at <https://doi.org/10.1038/s42003-025-07925-z>.

**Correspondence** and requests for materials should be addressed to Yinliang Wang or Bingzhong Ren.

**Peer review information** *Communications Biology* thanks Julien Brechbühl and the other, anonymous, reviewer(s) for their contribution to the peer review of this work. Primary Handling Editors: Michele Repetto. A peer review file is available.

**Reprints and permissions information** is available at <http://www.nature.com/reprints>

**Publisher's note** Springer Nature remains neutral with regard to jurisdictional claims in published maps and institutional affiliations.

**Open Access** This article is licensed under a Creative Commons Attribution-NonCommercial-NoDerivatives 4.0 International License, which permits any non-commercial use, sharing, distribution and reproduction in any medium or format, as long as you give appropriate credit to the original author(s) and the source, provide a link to the Creative Commons licence, and indicate if you modified the licensed material. You do not have permission under this licence to share adapted material derived from this article or parts of it. The images or other third party material in this article are included in the article's Creative Commons licence, unless indicated otherwise in a credit line to the material. If material is not included in the article's Creative Commons licence and your intended use is not permitted by statutory regulation or exceeds the permitted use, you will need to obtain permission directly from the copyright holder. To view a copy of this licence, visit <http://creativecommons.org/licenses/by-nc-nd/4.0/>.

© The Author(s) 2025